

HUMAN & MOUSE CELL LINES

Engineered to study multiple immune signaling pathways.

Transcription Factor, PRR, Cytokine, Autophagy and COVID-19 Reporter Cells
ADCC, ADCC and Immune Checkpoint Cellular Assays



The Journal of Immunology

RESEARCH ARTICLE | NOVEMBER 15 2019

RelB Deficiency in Dendritic Cells Protects from Autoimmune Inflammation Due to Spontaneous Accumulation of Tissue T Regulatory Cells

Nico Andreas; ... et. al

J Immunol (2019) 203 (10): 2602–2613.

<https://doi.org/10.4049/jimmunol.1801530>

Related Content

Impairment of Mature B Cell Maintenance upon Combined Deletion of the Alternative NF- κ B Transcription Factors RELB and NF- κ B2 in B Cells

J Immunol (March,2016)

Essential Role of RelB in Germinal Center and Marginal Zone Formation and Proper Expression of Homing Chemokines

J Immunol (August,2001)

Both multiorgan inflammation and myeloid hyperplasia in RelB-deficient mice are T cell dependent.

J Immunol (November,1996)

RelB Deficiency in Dendritic Cells Protects from Autoimmune Inflammation Due to Spontaneous Accumulation of Tissue T Regulatory Cells

Nico Andreas,^{*,†,1} Maria Potthast,^{‡,1} Anna-Lena Geiselhöringer,^{‡,1} Garima Garg,[§] Renske de Jong,[‡] Julia Riewaldt,^{¶,2} Dennis Russkamp,[‡] Marc Riemann,^{*} Jean-Philippe Girard,^{||} Simon Blank,[‡] Karsten Kretschmer,[¶] Carsten Schmidt-Weber,^{‡,#} Thomas Korn,^{§,**} Falk Weih,^{*,3} and Caspar Ohnmacht[‡]

Foxp3⁺ regulatory T cells are well-known immune suppressor cells in various settings. In this study, we provide evidence that knockout of the *relB* gene in dendritic cells (DCs) of C57BL/6 mice results in a spontaneous and systemic accumulation of Foxp3⁺ T regulatory T cells (Tregs) partially at the expense of microbiota-reactive Tregs. Deletion of *nfk2* does not fully recapitulate this phenotype, indicating that alternative NF- κ B activation via the RelB/p52 complex is not solely responsible for Treg accumulation. Deletion of RelB in DCs further results in an impaired oral tolerance induction and a marked type 2 immune bias among accumulated Foxp3⁺ Tregs reminiscent of a tissue Treg signature. Tissue Tregs were fully functional, expanded independently of IL-33, and led to an almost complete Treg-dependent protection from experimental autoimmune encephalomyelitis. Thus, we provide clear evidence that RelB-dependent pathways regulate the capacity of DCs to quantitatively and qualitatively impact on Treg biology and constitute an attractive target for treatment of autoimmune diseases but may come at risk for reduced immune tolerance in the intestinal tract. *The Journal of Immunology*, 2019, 203: 2602–2613.

Regulatory T cells (Tregs) expressing the master transcription factor Foxp3 have been described as key cells for the regulation of otherwise exaggerated and potentially fatal immune responses, both to foreign- and self-antigens. More recently, it became apparent that Tregs operate in different flavors depending on coexpression of master transcription factors, cytokine, and chemokine receptors typically associated with other Th cell subsets (1). For instance, Foxp3⁺ Tregs coexpressing the RAR-related orphan receptor γ t [ROR(γ t)] describe a population of Tregs in the intestinal lamina propria that is induced only by colonization with commensal bacteria (2, 3). Likewise, T-bet-expressing Tregs prevent severe Th1-dominated

autoimmunity, possibly due to colocalization with T-bet⁺ effector T (Teff) cells (4, 5). Combined deletion of both T-bet and Gata3 in Tregs has been shown to result in a spontaneous autoimmune disorder, whereas deletion of Gata3 alone prevents Treg stability under inflammatory conditions (6, 7). Typically, Tregs derived from nonlymphoid tissues such as skin or adipose tissue show a remarkable expression of genes previously associated to type 2 immunity, including *Il1rl1* and *Gata3*, and have been termed tissue Tregs (8–10). Local Tregs have been shown to play a key role for tissue integrity because Treg-intrinsic defects can result in reduced tissue function upon damage (11, 12). Thus, type 2 immune-biased Tregs may exert a similar

*Research Group Immunology, Leibniz Institute on Aging – Fritz Lipmann Institute, 07745 Jena, Germany; [†]Institute of Immunology, Jena University Hospital, 07743 Jena, Germany; [‡]Zentrum Allergie und Umwelt, Technische Universität und Helmholtz Zentrum München, 85764 Neuherberg, Germany; [§]Klinikum Rechts der Isar, Neurologische Klinik, Technische Universität München, 81675 Munich, Germany; [¶]Molecular and Cellular Immunology/Immune Regulation, German Research Foundation – Center for Regenerative Therapies Dresden, Center for Molecular and Cellular Bioengineering, Technical University Dresden, 01307 Dresden, Germany; ^{||}Institut de Pharmacologie et de Biologie Structural, Université de Toulouse, CNRS, UPS, 31077 Toulouse, France; [#]German Center for Lung Disease, 35392 Giessen, Germany; and ^{**}Munich Cluster for Systems Neurology, 81377 Munich, Germany

¹N.A., M.P., and A.-L.G. contributed equally to this work.

²Current address: Cellex Patient Treatment GmbH, Dresden, Germany.

³Deceased.

ORCIDs: 0000-0002-4591-7037 (N.A.); 0000-0001-7933-9426 (M.P.); 0000-0002-3633-0955 (T.K.).

Received for publication November 19, 2018. Accepted for publication September 9, 2019.

T.K. is supported by Deutsche Forschungsgemeinschaft Grants SFB1054-B6 and TR128-A7, the Federal Ministry of Education and Research – Germany (Tuberculosis in Neuromyelitis), and European Research Council Grant ERC-CoG EXODUS. F.W. has been supported by Deutsche Forschungsgemeinschaft Grants WE 2224/6 and WE 2224/6-2. C.O. is supported by the European Research Council of the European Union's Horizon 2020 Framework Program (Starting Grant ERC-StG 716718) and by the Deutsche Forschungsgemeinschaft (within FOR2559 - OH 282/1-1).

N.A., M.P., and A.-L.G. performed experiments and analyzed data with the help of G.G., R.d.J., M.R., and C.O. D.R. produced soluble ST2 and helped with experiments. J.R. and K.K. helped with in vivo experiments. J.-P.G. provided essential mouse strains. S.B., C.S.-W., and T.K. helped with specific analysis. F.W. initiated the study, N.A., M.P., and C.O. conceived the study, and C.O. wrote the manuscript. All authors discussed and approved the manuscript.

The RNA-sequencing data presented in this article have been submitted to the National Center for Biotechnology Information's Gene Expression Omnibus (<https://www.ncbi.nlm.nih.gov/geo/query/acc.cgi?acc=GSE134779>) under accession number GSE134779.

Address correspondence and reprint requests to Dr. Caspar Ohnmacht, Zentrum Allergie und Umwelt, Technische Universität und Helmholtz Zentrum München, Building 57, Room 103, Ingolstaedter Landstraße 1, 85764 Neuherberg, Germany. E-mail address: caspar.ohnmacht@helmholtz-muenchen.de

The online version of this article contains supplemental material.

Abbreviations used in this article: cDC, conventional DC; DC, dendritic cell; EAE, experimental autoimmune encephalomyelitis; MHC-II, MHC class II; mTEC, medullary thymic epithelial cell; PEC, peritoneal cavity; ROR(γ t), RAR-related orphan receptor γ t; sST2, soluble ST2; Teff, effector T; Treg, regulatory T cell; WT, wildtype.

This article is distributed under The American Association of Immunologists, Inc., [Reuse Terms and Conditions for Author Choice articles](#).

Copyright © 2019 by The American Association of Immunologists, Inc. 0022-1767/19/\$37.50

role as steady-state innate type 2 immunity in tissue homeostasis and repair (13). However, little is known about the cell-extrinsic mechanisms that imprint a tissue Treg phenotype into T cells.

APCs and notably dendritic cells (DCs) are well known for their capacity to initiate adaptive immune responses, whereas their role for tissue homeostasis and immune tolerance has been recognized only in recent years. For instance, conditional ablation of DCs leads to aggravated autoimmunity in a murine model of multiple sclerosis termed experimental autoimmune encephalomyelitis (EAE) (14). Furthermore, DCs are able to regulate tissue-resident Tregs both during thymic differentiation and by local activation (15). Constitutive ablation of DCs did initially not reveal a major impairment of thymic-derived Treg development but leads to a potentially autoimmune myeloproliferative disorder due to a defect in central tolerance (16, 17). By contrast, the absence of DCs but not myeloid cells impairs the generation of ROR(γ)⁺ Tregs and oral tolerance induction (2, 18). Thus, DCs have the capability to shape Treg biology in various settings.

In this study, we propose that expression of the noncanonical NF- κ B pathway member RelB but not NF- κ B2 in DCs has a dominant role in limiting the accumulation of Tregs with a tissue Treg signature. By contrast, commensal-induced ROR(γ)⁺ Tregs and induction of oral tolerance are reduced after ablation of RelB in DCs. We further show that such type 2 immune-biased Tregs are functional *in vitro* and *in vivo* and that accumulation of tissue Tregs is independent of nonhematopoietic IL-33 expression. Finally, mice lacking RelB expression in DCs are almost resistant to induction of autoimmune inflammation in the CNS in the EAE model. Thus, inactivation of the noncanonical NF- κ B member RelB in DCs leads to an accumulation of tissue Tregs and alters the ratio between self- versus foreign-reactive Tregs with consequences for different disease entities.

Materials and Methods

Mice

The following mouse strains were used: RelB^{KO/KO} (19), NF- κ B2^{KO/KO} (20), IL-33-LacZ gene-trap (IL-33^{Gt/Gt}) knockouts (21) Foxp3.gfp knock-in (Foxp3^{tm1Kueh}) mice (22) intercrossed to MOG TCR-specific 2D2 (Tg [Tera2D2, Terb2D2]^{1Kuc} [23]), and OT-II mice (Tg[TeraTcrb]425Cbn) (24) with the congenic marker CD45.1 (B6.SJL-Ptprc^a Pepc^b) were used as organs donors for adoptive transfer experiments. Mice expressing a DC-specific Cre recombinase (Tg[Itgax-cre]^{1-Reiz}) mice (25) were purchased at The Jackson Laboratory and crossed with mice carrying a loxP-flanked exon 4 of the *relb* gene (RelB^{fl/fl}) (19) to achieve deletion of *relb* in DCs (called RelB^{ADC} throughout the manuscript) or mice carrying a loxP-flanked exon 1 and 2 (NF- κ B2^{fl/fl}) (26) to achieve deletion of *nfk2* in DCs (called NF- κ B2^{ADC} throughout the manuscript). RelB^{fl/fl} mice were crossed to Foxp3 promoter-driven BAC transgenic Cre mice (27) to generate Treg-specific RelB deletion or to a Foxn1-driven Cre transgenic mouse line (28) to generate medullary thymic epithelial cell (mTEC)-specific RelB deletion (19). For cell sorting experiments, RelB^{ADC} were intercrossed to Foxp3^{tm1Flv} (29) reporter mice. Treg-deficient scurfy mice (Foxp3^{sf} [30]) were used at an age of 6 d. Littermate controls were used whenever possible. All mouse strains were backcrossed to a C57BL/6 background for at least 10 generations unless otherwise stated. Soluble sST2 (sST2) was injected three times per week at a dose of 100 μ g in PBS *i.p.* for a total of 3 wk into adult mice. All animals were kept under specific pathogen-free conditions. All interventions were performed in accordance with the European Convention for Animal Care and Use of Laboratory Animals and were approved by the local ethics committee and appropriate government authorities.

Induction of EAE

EAE was induced by injection of 200 μ l of an emulsion containing 200 μ g of MOG₃₅₋₅₅ peptide (MEVGWYRSPFSRVVHLYRNGK) and 500 μ g of *Mycobacterium tuberculosis* H37Ra (BD Difco) in CFA *s.c.* at the base of tail. On day 0 and 2 after immunization, mice received 200 ng of pertussis

toxin (Sigma). Alternatively, EAE was induced using a kit from Hooke laboratories according to the manufacturer's instructions. Clinical signs of disease were monitored according to the following scheme: score 1, tail paralysis; score 2, hind limb impairment; score 3, hind limb paralysis; score 4, front limb paralysis; score 5, death. In case hind limb movement was strongly impaired, mice were provided with a HydroGel H₂O and easily accessible wet food. For analysis of cytokine-producing T cells at peak of disease, lymphocytes were recovered from brains and spinal cords. Restimulation was either performed with MOG₃₅₋₅₅ peptide or PMA/ionomycin for 4 h. For the last 2 h, brefeldin A was added to the restimulated cells. When indicated, Tregs were ablated by *i.p.* injection of 500 μ g of anti-CD25 Ab (clone PC61; BioXCell) on days -5 and -3 prior to MOG₃₅₋₅₅ immunization. For transfer experiments 2.5 \times 10⁶ sort-purified Foxp3/GFP⁺ 2D2⁺ Th cells were injected *i.v.* 24 h prior to MOG₃₅₋₅₅ immunization. The induction of MOG-specific 2D2⁺Foxp3/GFP⁺ Tregs was analyzed by flow cytometry at day 7 after MOG₃₅₋₅₅ immunization in inguinal lymph nodes.

Rescue of scurfy mice

A total of 2 \times 10⁶ sort-purified CD4⁺ splenocytes from wildtype (WT) or RelB^{ADC} mice were injected *i.p.* into 3–6-d-old Foxp3^{KO/KO} (Scurfy) mice. Nontreated Scurfy mice did not receive any cells. Survival and body weight were monitored for 60 d after cell transfer.

OT-II cell transfer and OVA feeding

Naive T cells from spleens and lymph nodes of OTII/CD45.1 mice were sort-purified or isolated by magnetic separation using a naive CD4⁺ T cell isolation kit (Miltenyi Biotec), and 0.5 \times 10⁶ naive OT-II T cells were injected *i.v.* into WT and RelB^{ADC} recipients. Upon transfer mice were fed with 1.5% OVA fraction V (Sigma-Aldrich) in drinking water *ad libitum* for 9 d before analysis.

Bone marrow chimeras

Recipient mice were lethally irradiated by a Co-60 source with two doses of 6 Gy 4 h apart. Irradiated mice were reconstituted with 8 \times 10⁶ purified bone marrow cells of respective donors by *i.v.* injection. After reconstitution, mice received 0.25 mg/ml Enrofloxacin (Baytril; Bayer Vital GmbH) in drinking water for 3 wk. Bone marrow chimeras were analyzed 10–12 wk after reconstitution.

Production and use of sST2

sST2 cDNA (amino acids 1–337) was designed and ordered at Invitrogen Strings. A total of 5 μ l of DNA fragment (20 ng/ μ l) were digested with NheI and XhoI, and digested fragment was gel-purified using the GeneJET Gel extraction kit according to manufacturer's instructions. Purified fragments were ligated with dephosphorylated NheI and XhoI digested pcDNA3.1 using T4 DNA ligase (NEB). Competent XL10 gold cells were transformed with the ligation mix according to manufacturer's guidelines and plated on agar plates containing 100 μ g/ml ampicillin. Selected colonies were picked, and plasmids were isolated using the GeneJET plasmid prep mini kit and sequenced. Plasmids from a clone with the correct sequence were used to transfect Hek293 cells with Lipofectamine 3000 Reagent (Thermo Fisher Scientific). To generate stable cell lines, transfected cells were cultured in complete RPMI in presence of G418 for 4 wk. Presence of sST2 in the supernatant was confirmed by Western blot using a polyclonal goat anti-sST2 Ab (Abcam) and ELISA (R&D Systems). For large-scale production of sST2, supernatant of sST2-producing cells was affinity purified via His tag using nickel columns (HisTrap excel). sST2 was further purified using size-exclusion chromatography (HiLoad 16/600 Superdex 75 μ g).

Biological activity of sST2 was proven according to standard protocols. Briefly, murine splenocytes were cultured in the presence of activating CD3/CD28 Abs in the presence of 10 ng/ml IL-33 (PeproTech). Addition of sST2 entirely suppressed the IL-33-induced production of IL-5 in a dose-dependent manner (data not shown).

Preparation of CNS mononuclear cells

At the peak of EAE, mice were sacrificed and perfused immediately with 10 ml of cold PBS through the left cardiac ventricle after opening the right ventricle. Brains and spinal cords were removed, cut into small pieces, and digested for 45 min at 37°C in 2.5 mg/ml collagenase D and 1 mg/ml DNase in DMEM. The digestion preparation was homogenized through a 70- μ m cell strainer and centrifuged at 400 \times g for 10 min. The cell pellet was resuspended in 30% Percoll and layered onto 70% Percoll. Percoll gradient was run at 1800 \times g for 20 min without break, and the interphase containing mononuclear cells was collected for further analysis.

Isolation of gut lamina propria cells

Lamina propria of small intestine was prepared as described (2). Briefly, small intestine was flushed with PBS, and Peyer patches were removed. Intestines were cut longitudinally and incubated in 30 mM EDTA in PBS at pH 8 on ice for 30 min. Thereafter, tissues were vigorously washed in PBS repeatedly, minced into small pieces, and digested in RPMI containing 25 mM HEPES, 0.05 mg/ml collagenase D (Roche), and 10 μ g/ml DNase I (Sigma-Aldrich) at 37°C for 1 h with intermittent pipetting and replacement of digestion media. Collected supernatants were filtered through a 70- μ m cell strainer and centrifuged at 500 \times *g* for 10 min. The cell pellet was resuspended in a 40% Percoll (GE Healthcare) solution and layered onto an 80% Percoll layer. The Percoll gradient was run at 1500 \times *g* at room temperature for 15 min. The interlayer containing lamina propria mononuclear cells was collected and washed prior to further analysis.

Flow cytometry and cell sorting

Single-cell suspensions were prepared by digestion with collagenase D and DNase I, mechanical organs disruption, or peritoneal lavage, incubated with Fc blocking Ab (BD) and stained with the corresponding Abs on ice. Intracellular staining was performed using a Foxp3 fixation/permeabilization kit (eBiosciences) according to the manufacturer's instructions. Live/Dead exclusion was routinely performed using a kit from Life Technologies, and Tregs or Teff cells were identified as single cells as Live/Dead⁻ CD45⁺CD3⁺CD4⁺Foxp3⁺ or Live/Dead⁻ CD45⁺CD3⁺CD4⁺Foxp3⁻ cell, respectively. Conventional DCs (cDCs) were identified as Live/Dead⁻, CD45⁺ cells expressing high levels of MHC class II (MHC-II), and CD11c. Cell sorting was performed with a FACSAria III cell sorter (BD), and cell purity was typically around 99%. For data analysis FlowJo V7.5.2 (Tree Star) software was used.

Treg suppression assay

MHC-II⁺ CD11c^{high} DCs were isolated from spleens of control mice and cocultured with CFSE-labeled CD4⁺CD62L⁺CD44^{low} naive Th cells isolated from control spleens in presence of 1 μ g/ml soluble anti-CD3 for 3 d in a 96-well plate. If indicated, Tregs from control or RelB^{ADC} spleens were cocultured at a 1:2 ratio. Ratio of T cells to DCs was 5:1 with 1 \times 10⁵ T cells per well.

ELISA

Sandwich ELISA for total serum IgE was performed using a polyclonal sheep anti-mouse IgE (The Binding Site) for coating and biotinylated rat anti-mouse IgE (clone R35-118; BD Biosciences) for detection. After incubation with streptavidin-peroxidase (Calbiochem), tetramethylbenzidine (Fluka) was used according to the manufacturer's instructions, and absorption was measured at 450 nm. IL-2 and IL-33 serum levels were measured with a multiplex assay (Meso Scale Diagnostics) according to the manufacturer's instructions.

RNA-sequencing analysis

Total RNA was extracted from sort-purified Tregs from RelB^{ADC}Foxp3^{RFP} mice from indicated organs using a RNeasy Micro Kit (Qiagen). Complete cDNA was synthesized from 5 μ l of total RNA using the SmartScribe reverse transcriptase (Takara Bio) with a universally tailed poly-dT primer and a template-switching oligo followed by amplification for 12 cycles with the Advantage 2 DNA Polymerase (Takara Bio). After ultrasonic shearing (LE220; Covaris), amplified cDNA samples were subjected to standard Illumina fragment library preparation using the NEBnext Ultra DNA library preparation chemistry (New England Biolabs). In brief, cDNA fragments were end-repaired, A-tailed, and ligated to indexed Illumina TruSeq adapters. Resulting libraries were PCR amplified for 15 cycles using universal primers, purified using XP beads (Beckman Coulter), and then quantified with the Fragment Analyzer. Final libraries were equimolarly pooled and subjected to 75-bp single-end sequencing on the Illumina NextSeq 500 platform, resulting in ~27–47 mio reads. Reads were mapped to the mouse genome (version mm10) with GSNAP ([31]; v2018-03-11) and splice sites from Ensembl (version 81) as support. RNA-sequencing (RNA-seq) data quality was assessed with RNA-SeQC ([32]; v1.1.8). Uniquely mapped reads served as input for obtaining gene counts with featureCounts ([33]; v1.6.0) and Ensembl gene annotations (version 81). Principle component analysis and visualization was done in R using prcomp and ggplot functions. Normalization for library size and identification of differentially expressed genes was done with the R package DESeq2 ([34]; v1.18.1). DESeq2 *p* values were adjusted for multiple testing (Benjamini-Hochberg), and genes with an adjusted *p* value < 0.1 were

considered as differentially expressed. RNA-sequencing data of this study are available at the National Center for Biotechnology Information's Gene Expression Omnibus database under accession number GSE134779 (<https://www.ncbi.nlm.nih.gov/geo/query/acc.cgi?acc=GSE134779>).

Statistics

Data were analyzed by two-tailed Student *t* test and, unless otherwise indicated, analyzed using GraphPad Prism software. Bar diagrams show mean \pm SD unless otherwise indicated. Mann-Whitney *U* test and two-way ANOVA with Tukey multiple correction test were used in EAE experiments as indicated. Statistical significance was set at: **p* < 0.05, ***p* < 0.01, ****p* < 0.001, and *****p* < 0.0001.

Results

NF- κ B members alter Foxp3⁺ regulatory T cells in a DC-specific manner

Complete knockout of the noncanonical NF- κ B member RelB has been shown to result in severe T cell-dependent autoimmune inflammation (35–37). In most cell types, RelB typically pairs with p52, a breakdown product of NF- κ B2/p100, to mediate signaling via the so-called alternative NF- κ B pathway. Therefore, we first addressed whether genetic deletion of RelB or the regulatory element of the p100/NF- κ B2 precursor protein (20) alters systemic Treg homeostasis. Confirming earlier observations, RelB deficiency resulted in a drastic increase of Foxp3⁺ Tregs in the spleen (Fig. 1A). Surprisingly, bone marrow chimeras receiving p100-deficient bone marrow did not show any alteration in Foxp3⁺ Tregs (Fig. 1A). To investigate a potential role of RelB or NF- κ B2 in DCs for Treg biology, we crossed mice with a floxed allele of the *relb* gene (19) or *nfk2* gene (26) to mice expressing the *Cre* recombinase under control of a DC-specific promoter (25) called RelB^{ADC} or NF- κ B2^{ADC} mice, respectively. We first checked deletion efficacy in different cellular subsets of the spleen and bone marrow-derived macrophages. As expected, splenic DCs showed the most efficient *relb* deletion (Supplemental Fig. 1A) compared with other splenic subsets. Bone marrow-derived macrophages also partially deleted RelB (Supplemental Fig. 1A), indicating at least modest expression of CD11c and recombination in other myeloid lineages. Still, in this manuscript we will continue to talk about DCs for consistency with the current literature related to Itgax-Cre line. Interestingly, RelB^{ADC} mice showed a similar increase in splenic Tregs as complete RelB-deficient mice, whereas NF- κ B2^{ADC} mice showed only a modest yet significant increase in Treg numbers (Fig. 1B). To definitively exclude a Treg-intrinsic role of RelB, we additionally ablated RelB exclusively in Foxp3⁺ Tregs. We did not find any difference in Treg numbers of mice lacking RelB in Foxp3⁺ cells (Fig. 1B) in line with recent findings for a T cell-extrinsic role of RelB in the regulation of Treg biology (38, 39). As both canonical and noncanonical NF- κ B pathways regulate DC activation and maturation in an interactive manner (40), we addressed how splenic DCs are altered in the absence of RelB or NF- κ B2. Conditional ablation of RelB but not NF- κ B2 resulted in a slight reduction of overall DC frequencies and a relative increase of Sirp α ⁻CD8 α ⁺ DCs that expressed high levels of DEC-205 (Fig. 1C, 1D). This confirms earlier results in which RelB has been shown to be necessary for the development of splenic myeloid-related CD8 α ⁻ DCs (cDC2s) (41–43). DEC-205 has been previously associated to Treg induction, and the relative increase of DEC-205⁺ DCs in RelB^{ADC} but not in NF- κ B2^{ADC} mice may contribute to Treg accumulation (Fig. 1C, 1D and [44]). Besides DEC-205, altered expression patterns of costimulatory molecules on DCs may contribute to Treg accumulation in RelB^{ADC} mice. Indeed, DCs from RelB^{ADC} expressed less PD-L1 but more PD-L2, whereas expression of OX40L remained unchanged relative to control animals at steady-state (Fig. 1E).

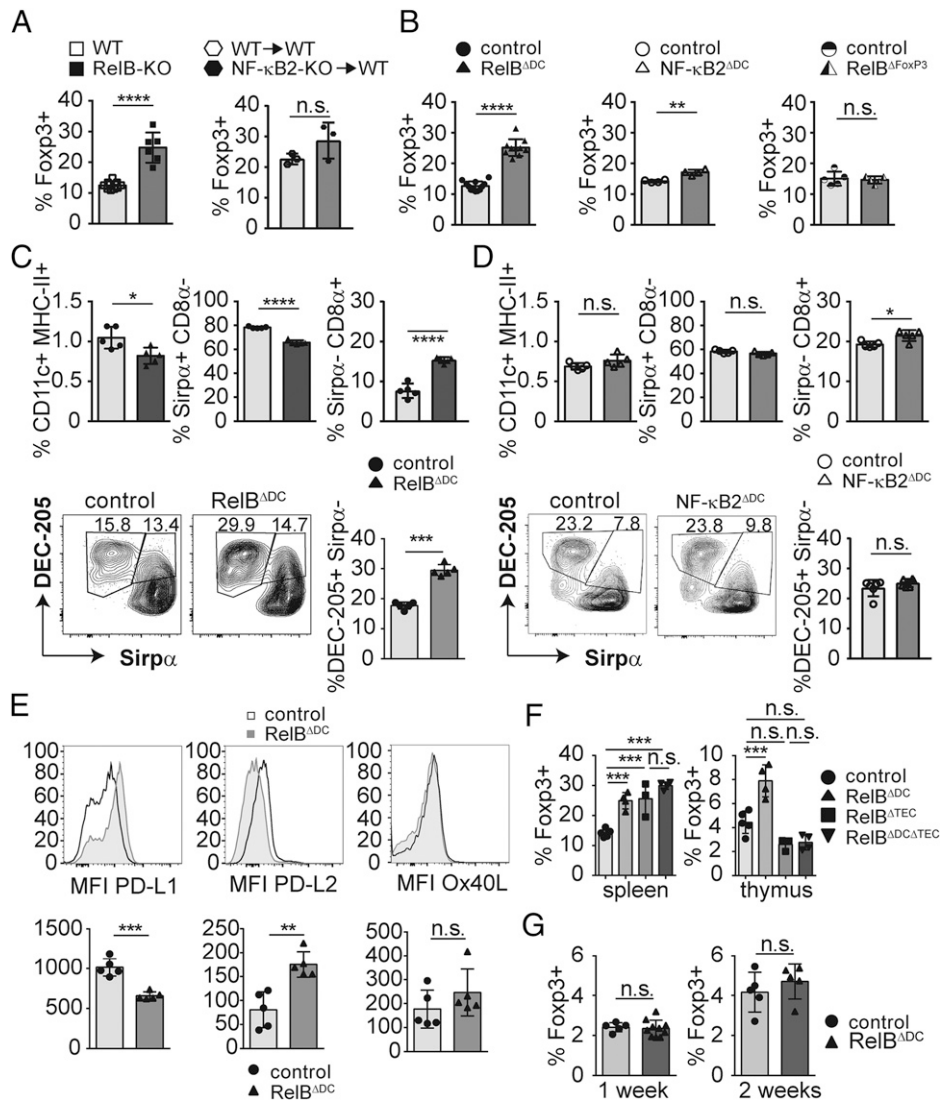


FIGURE 1. Differential impact of alternative NF-κB member on DCs and Tregs. Frequencies of F_{oxp3}⁺ Tregs among CD4⁺ T cells in spleens of the indicated knockout animals or bone marrow chimeras. **(A)** Frequencies of F_{oxp3}⁺ Tregs among CD4⁺ T cells in spleens of the indicated conditional knockout animals. **(B)** Frequencies of F_{oxp3}⁺ Tregs among CD4⁺ T cells in spleens of the indicated conditional knockout animals. **(C)** Bar diagrams show frequencies of splenic DCs and Sirpα⁺CD8α⁻ and Sirpα⁻CD8α⁺ DC subsets (upper panels) of control and RelB^{ADC} mice. Contour plots (lower panels) show DEC-205⁺Sirpα⁻ splenic DC subsets and enumeration in control and RelB^{ADC} mice. **(D)** Bar diagrams show frequencies of splenic DCs and Sirpα⁺CD8α⁻ and Sirpα⁻CD8α⁺ DC subsets (upper panels) of control and NF-κB2^{ADC} mice. Contour plots (lower panels) show DEC-205⁺Sirpα⁻ splenic DC subsets and enumeration in control and NF-κB2^{ADC} mice. **(E)** Representative histograms and mean fluorescence intensity (MFI) of PD-L1, PD-L2, and OX40L expression on dendritic cells (CD11c⁺MHC-II⁺) in spleens from littermate control (filled histogram) or RelB^{ADC} mice (open histograms). **(F)** Quantification of F_{oxp3}⁺ Treg frequencies in spleen and thymus of WT or RelB^{ADC} mice or mice lacking RelB in medullary thymic epithelial cells (RelB^{ATEC}) or both (RelB^{ADC}ATEC). Statistics were performed with one-way ANOVA with Tukey multiple correction test (***p* < 0.001). **(G)** Quantification of Treg frequencies in the thymi of 1-week and 2-week-old littermate controls and RelB^{ADC} mice. All data show pooled results of at least two independent experiments and if not stated differently, analyzed by two-tailed Student *t* test. Bar diagrams show mean ± SD. **p* < 0.05, ***p* < 0.01, ****p* < 0.001, *****p* < 0.0001.

Thus, signaling via the NF-κB member RelB but not NF-κB2/p52 in DCs has a dominant role in controlling Treg homeostasis.

Enhanced differentiation of Tregs in the thymus could alternatively account for an accumulation of peripheral Tregs. Indeed, we found more F_{oxp3}⁺ Tregs in the thymus of adult RelB^{ADC} mice (Fig. 1F). We also observed a slight reduction of thymic Sirpα⁺ DCs in RelB^{ADC} but not NF-κB2^{ADC} mice similar to splenic DCs lacking RelB (Supplemental Fig. 1B and [42, 43]). Given that migration of peripheral Sirpα⁺CD8^{lo} DCs to the thymus has been proposed to efficiently induce Treg differentiation (45, 46) the observed reduction of this DC subset in the thymus of RelB^{ADC} mice makes it unlikely that peripheral DCs contribute to thymic Treg accumulation. In line with decreased Treg frequencies in

RelB^{ATEC} mice (19), simultaneous ablation of RelB in DCs and mTECs prevented increased Treg frequencies in the thymus of adult mice compared with control mice, whereas Treg numbers in spleen were still increased (Fig. 1F). Treg accumulation in spleens of RelB^{ADC}ATEC mice may be due to altered negative selection in RelB^{ATEC} mice resulting in autoimmunity (19) and a dominant effect of RelB-deficient DCs in the periphery. As peripherally induced Tregs can migrate to the adult thymus (47), we measured Treg frequencies in very young mice, in which peripheral Treg conversion is still very limited. However, we did not observe an increase in thymic Treg frequencies at 1 or 2 wk of age (Fig. 1G). Finally, conversion of otherwise negatively selected T cells into the Treg lineage can equally result in enhanced Treg differentiation in

the adult thymus. To test this hypothesis, we crossed RelB^{ADC} mice on a C57BL/6 background for one generation to a BALB/c background in which a superantigen encoding retrovirus is exclusively expressed in DCs (Mtv-6). This results in impaired negative selection of Vβ3⁺ T cells in the constitutive absence of DCs (16). However, we did not find any difference among Vβ3⁺ Tregs between C57BL/6 and mixed background mice in the absence of RelB in DCs (Supplemental Fig. 1C). In summary, these results indicate that accumulation of Tregs in RelB^{ADC} mice depends on age-dependent peripheral differentiation of Tregs by DC-intrinsic effects induced by the absence of RelB-dependent gene regulation.

Accumulated Tregs in RelB^{ADC} mice show a tissue Treg signature

As our results so far indicate an accumulation of Tregs by peripheral mechanisms, we performed a detailed characterization of Tregs in several tissues of RelB^{ADC} and NF-κB2^{ADC} mice. All examined organs showed an accumulation of Foxp3⁺ Tregs in RelB^{ADC} and RelB^{KO/KO} mice, and this was particularly pronounced among Helios⁺ Tregs (Fig. 2A, Supplemental Fig. 2A, 2B and data not shown). This effect was almost completely blunted in NF-κB2^{ADC} mice (Fig. 2A, Supplemental Fig. 2A), indicating that Treg accumulation occurred in a RelB-dependent but NF-κB2-independent fashion. The high expression levels of Helios among accumulated Tregs in RelB^{ADC} and NF-κB2^{ADC} mice argues for a preferential accumulation of Tregs specific for self-antigens because thymic and tissue-restricted neo-self-antigens have been shown to induce Tregs that express Helios (48, 49). As increased proliferation rates may contribute to Treg accumulation, we measured intracellular Ki-67 expression among Tregs of various organs. Indeed, we found higher Ki-67 expression in Tregs in spleen and lymph nodes but not thymus of RelB^{ADC} compared with control mice (Fig. 2B).

To gain deeper insight into the identity of accumulated Tregs in RelB^{ADC} mice, we performed RNA-seq analysis of sort-purified Tregs from RelB^{ADC} mice backcrossed to a Foxp3 reporter line. Indeed, Tregs derived from the peritoneal cavity (PEC) as one of the sites with the highest Treg accumulation revealed a number of differently expressed genes reminiscent of tissue Tregs in RelB^{ADC} mice, including high expression levels of *Klrg1*, *Il1rl1*, *Gata3*, *Pparg*, *Itgae*, *Nrpl*, and *Tnfrsf4* but low expression of *Bcl2* and *CCR7* (Fig. 2C, Supplemental Fig. 2C and [8]). We were able to confirm these Treg markers by flow cytometry, including KLRG1, OX40 (encoded by *Tnfrsf4*), CD103, PD-1, ICOS, GITR, and ST2 (encoded by *Il1rl1*) (Fig. 2D, Supplemental Fig. 2D). Interestingly, some of the tissue Treg signature genes were even found to be differentially expressed in Tregs isolated from the spleen and thymus of RelB^{ADC} mice, indicating a systemic shift in favor of tissue Tregs (Supplemental Fig. 2C). Expression of *Satb1*, a recently identified genome organizer necessary for proper Treg differentiation in the thymus upstream of Foxp3 expression (50), was expressed at lower levels in Tregs derived from RelB^{ADC} mice compared with controls in all organs (Fig. 2C, Supplemental Fig. 2C).

Barrier organs such as the intestinal tract are exposed to both self- and harmless foreign Ags that similarly rely on induction of Foxp3⁺ Tregs for maintenance of immune tolerance. We confirmed that accumulated Tregs in RelB^{ADC} mice expressed higher Gata3 levels within the intestinal tract, and this was again dominant among Helios⁺ Tregs (Fig. 2E). Surprisingly, microbiota-induced ROR(γt)⁺ Tregs in the small intestine were reduced in RelB^{ADC} mice (Fig. 2F) even when excluding accumulated Helios⁺ Tregs (Supplemental Fig. 2E). As ROR(γt)⁺ Tregs are able to regulate type 2 immunity (2), we tested whether a comparable

phenotype was observed in Teff cells of RelB^{ADC} mice. Indeed, Gata3⁺ Teff cells accumulated spontaneously in the intestinal tract of RelB^{ADC} mice (Fig. 2G). Whether accumulation of Gata3⁺ Th2 cells is a direct consequence of RelB deficiency in DCs or a result of the altered Treg compartment remains to be addressed. In line with these observations we found elevated levels of IgE in the serum and on the surface of FcεRI-bearing basophils and mast cells of RelB^{ADC} mice, a hallmark of type 2 immunity (Fig. 2H, Supplemental Fig. 3A, 3B). All of these observations could also be found in RelB^{KO/KO} mice (Supplemental Fig. 3D–F) and (37). Despite this systemic type 2 immune bias in T cells and a tendency of increased blood eosinophils levels in RelB^{ADC} mice (Supplemental Fig. 3C), we did not find any visible signs of inflammation typically observed in RelB^{KO/KO} mice (data not shown and [35–37]). Thus, both RelB^{KO/KO} and RelB^{ADC} mice show an accumulation of Gata3^{hi} tissue Tregs partially at the expense of ROR(γt)-expressing Tregs.

Tissue Tregs in RelB^{ADC} mice accumulate independent of IL-33

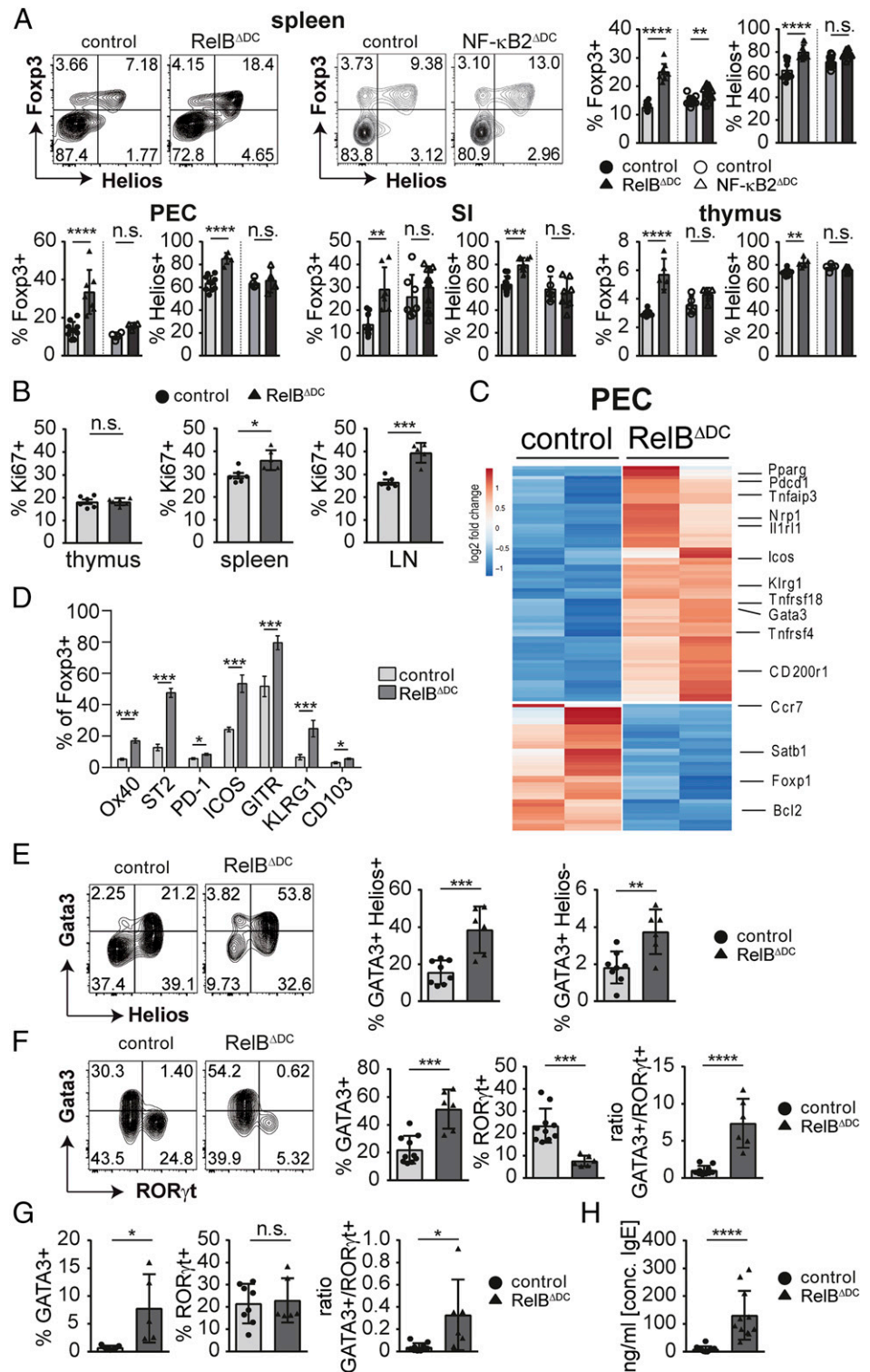
In line with the systemic type 2 immune bias in T cells from RelB^{ADC} mice, we also observed higher expression of the IL-33R ST2 on Gata3⁺ Teff cells and Helios⁺ Tregs (Fig. 3A, 3B). Notably, ST2 expression has been previously linked to high Gata3 expression in Tregs (51). Given that IL-2/anti-IL-2 Ab complexes and particularly external IL-33 administration can boost the accumulation of ST2⁺/Gata3⁺ Tregs (6, 51, 52), we asked whether excessive IL-2 or IL-33 could be one of the drivers for the accumulation of tissue Tregs in RelB^{ADC} mice (reviewed in Ref. 53). First, we did not find differences in serum levels of IL-33 nor IL-2 in the serum of RelB^{ADC} mice compared with control mice (Fig. 3C). In addition, blocking IL-33 by injection of a sST2 decoy receptor over 3 wk did not reveal a major difference in total or ST2⁺ Treg frequencies (Fig. 3D). As IL-33 is predominantly expressed by nonhematopoietic cells (21), we additionally created bone marrow chimeras with IL-33^{KO/KO} animals as recipients. Again, we found a similar increase in ST2⁺Helios⁺ Tregs and Th2-biased Teff cells compared with WT recipients receiving bone marrow from RelB^{ADC} mice despite undetectable IL-33 levels in IL-33^{KO/KO} recipients (Fig. 3E). Noteworthy is that constitutive IL-33-deficient mice possess normal levels of ST2⁺ Tregs (54). This may indicate that IL-33 expands Tregs to prevent tissue damage (e.g., during ongoing type 2 immune-driven inflammation) but is not the primary driver for the tissue Treg phenotype under physiologic conditions or in RelB^{ADC} mice. Additionally, these results rule out a role of nonhematopoietic RelB expression (e.g., by mTECs or other radio-resistant cells of nonhematopoietic origin [42]).

In summary, these results reveal that the increase in Tregs with a tissue Treg phenotype is independent of IL-33 or other nonhematopoietic effects. Several RelB-dependent mechanisms in DCs may be in place that regulate Treg biology in an integrative manner depending on the antigenic source and/or the anatomical site.

Tregs from RelB^{ADC} mice are functional in vitro and in vivo

The type 2 immune bias of the accumulated Tregs observed in RelB^{ADC} mice raised the question of whether these Tregs are still functional because Th2 reprogramming of Tregs after excessive IL-4 or IL-33 signaling and corresponding high Gata3 expression has been proposed to impair their tolerogenic function (52, 55). Therefore, we first cocultured Tregs derived from RelB^{ADC} or control mice with Teff cells in the presence of WT myeloid DCs. Under these in vitro settings, we did not find a difference in their suppressive capacity (Fig. 4A). Next, we tested whether Tregs

FIGURE 2. Accumulated Tregs in RelB^{ADC} mice show a tissue Treg signature with a type 2 immune bias. **(A)** Representative FACS plots and quantification of Foxp3⁺ Tregs among CD4⁺ T cells and frequency of Helios⁺ among total Tregs in indicated organs. Statistics were performed with one-way ANOVA with Tukey multiple correction test. **(B)** Bar diagrams show frequencies of Ki-67⁺ cells among Foxp3⁺ Tregs in indicated organs. **(C)** Heatmap depicts selected differentially expressed genes according to RNA-seq analysis of sort-purified Tregs isolated from the PEC of control or RelB^{ADC} mice with a false discovery rate < 0.1 and adjusted *p* < 0.1. **(D)** Quantification of selected tissue Treg marker expression in PEC by flow cytometry. **(E)** Representative FACS plots and quantification of Gata3^{hi}Helios⁺ and Gata3^{hi}Helios⁻ within pregated Foxp3⁺ Tregs isolated from the lamina propria of the small intestine. **(F)** Representative FACS plots (left) and bar diagrams (right) of RORγt and Gata3 expression within pregated Foxp3⁺ Tregs isolated from the lamina propria of the small intestine and ratio between Gata3 and RORγt-expressing Tregs. **(G)** Bar diagrams show frequencies of RORγt⁺ and Gata3^{hi} T cells among Foxp3⁻ Teff cells ratio between Gata3 and RORγt-expressing Teff cells isolated from the small intestine. **(H)** Concentration of total serum IgE level of naive adult mice. All data show pooled results of at least two independent experiments and analyzed, if not stated differently, by two-tailed Student *t* test. Bar diagrams show mean ± SD. **p* < 0.05, ***p* < 0.01, ****p* < 0.001, *****p* < 0.0001.



from each genotype are able to prevent wasting disease in mice carrying the *scurfy* mutation that results in severe autoimmune inflammation due to an intrinsic Treg deficiency. When reconstituted with Tregs from RelB^{ADC} or control mice, *scurfy* mice could be rescued equally with only minor variations in survival and weight gain (Fig. 4B). So far, these data indicate that Tregs from RelB^{ADC} mice are functional in vitro and in vivo. Finally, we also tested whether oral tolerance induction is enhanced in RelB^{ADC} mice. We transferred congenitally labeled naive OT-II cells into RelB^{ADC} or control mice and applied OVA via the

drinking water. Surprisingly, we found reduced frequencies of de novo-induced Tregs derived from naive OT-II cells in RelB^{ADC} mice, and these Tregs additionally expressed less ROR(γt) (Fig. 4C). As we have previously shown that microbiota-induced ROR(γt)⁺ Tregs are able to regulate Th2-dominated immune responses, we also looked for de novo differentiation of Th2 cells (2). Indeed, we found an upregulation of Gata3 both within the Treg and the Teff cell compartment in RelB^{ADC} mice (Fig. 4D, 4E). In summary, these results indicate that accumulated Tregs in RelB^{ADC} mice are functional and protect from inflammation.

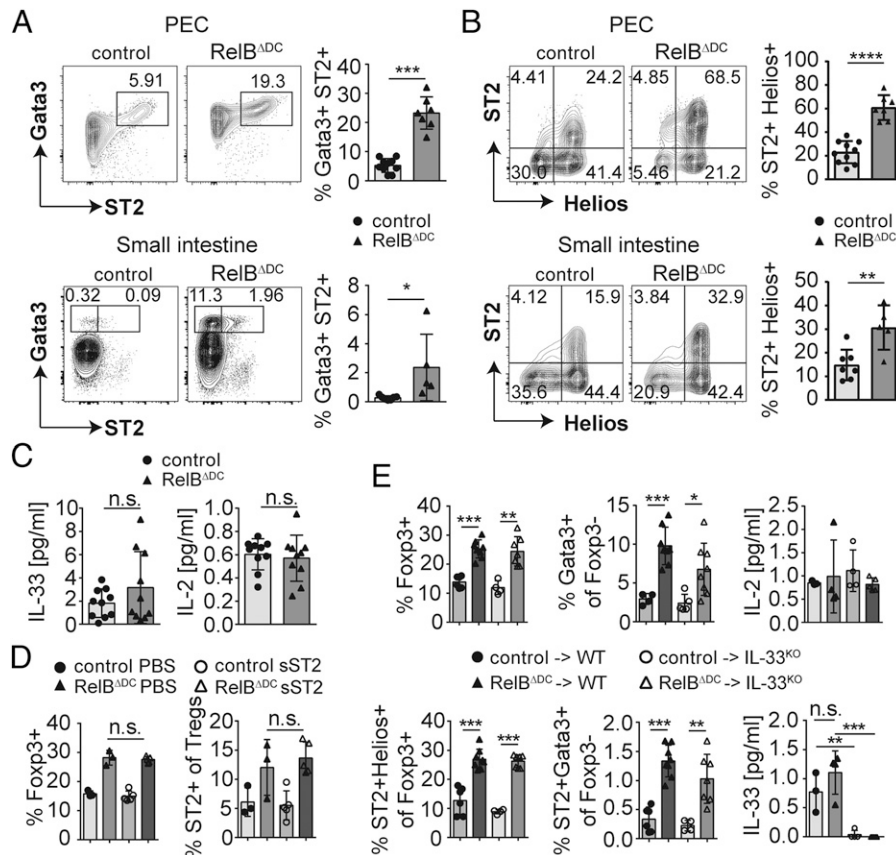


FIGURE 3. RelB^{ADC} mice accumulate ST2⁺ tissue Tregs independent of IL-33. **(A)** Representative FACS plots (left) and quantification (right) of Gata3⁺ST2⁺ cells within Fopx3⁺ T cells in PEC or small intestine of littermate control and RelB^{ADC} mice. **(B)** Representative FACS plots (left) and quantification (right) from littermate control and RelB^{ADC} mice showing ST2⁺ Helios⁺ cells among Fopx3⁺ Tregs from PEC and lamina propria of the small intestine. **(C)** IL-33 and IL-2 serum levels of control littermates and RelB^{ADC} mice. **(D)** sST2 or PBS was injected i.p. every other day into control or RelB^{ADC} mice for 3 wk. Bars indicate Fopx3⁺ Treg numbers and ST2 expression among Tregs in the spleen at the end of the experiment. Statistics were performed with one-way ANOVA with Tukey multiple correction test. **p* < 0.05, ***p* < 0.01, ****p* < 0.001, *****p* < 0.0001. **(E)** Treg frequencies and expression of Helios, ST2, and Gata3 in the spleen from bone marrow chimeras receiving either bone marrow from littermate or RelB^{ADC} animals. WT or IL-33^{KO/KO} animals served as recipients as indicated. Lower plots show serum levels of IL-33 or IL-2 in the described bone marrow chimeras. Statistics were performed with one-way ANOVA with Tukey multiple correction test. **p* < 0.05, ***p* < 0.01, ****p* < 0.001, *****p* < 0.0001. All data show pooled results of one (E) or at least two independent experiments and analyzed if not stated differently, by two-tailed Student *t* test. Bar diagrams show mean ± SD. **p* < 0.05, ***p* < 0.01, ****p* < 0.001, *****p* < 0.0001.

However, this occurs at the expense of impaired de novo Treg differentiation capacity and accumulating Th2 cells in the intestinal tract in response to foreign oral Ags similar to what has been found in germ-free mice (56).

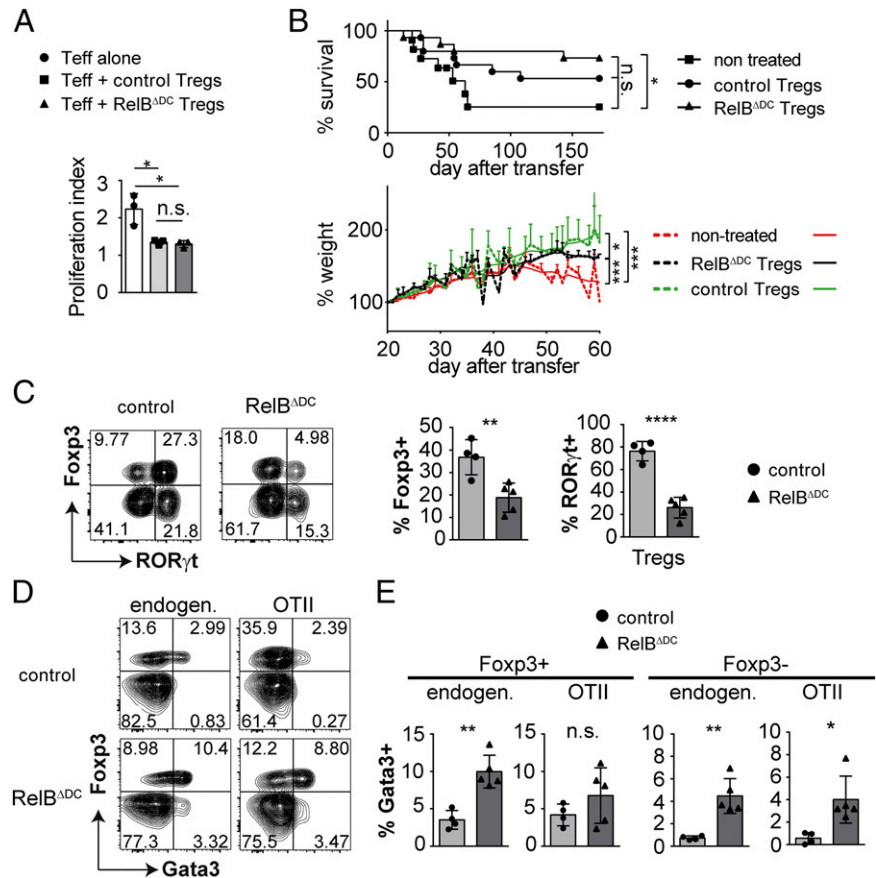
Accumulation of tissue Tregs protects from autoimmunity

Overall, our data indicate a specific accumulation of Tregs with a tissue Treg signature in RelB^{ADC} mice. Given that Gata3⁺ Tregs are still present in the absence of microbial stimulation by bacterial symbionts (2), we reasoned that most of the accumulated Tregs in RelB^{ADC} mice are specific for self-antigens and may thus protect from autoimmune inflammation. We therefore induced EAE in both RelB^{ADC} and control mice and followed disease scores. Intriguingly, RelB^{ADC} mice were almost completely protected from disease, whereas littermates showed severe signs of autoimmune inflammation (max. mean score: 2.4 [control] versus 0.58 [RelB^{ADC}]) [Fig. 5A]. In line with the low EAE scores we found reduced absolute numbers of pathogenic cytokine-producing T cells in the spinal cord (Fig. 5B, Supplemental Fig. 4A). Moreover, less of these infiltrating T cells were specific for MOG protein because restimulation with MOG_{35–55} peptide revealed reduced numbers of CD154⁺ Ag-specific T cells in the CNS of RelB^{ADC} mice (Supplemental Fig. 4B). We also found more Gata3⁺

T cells and Tregs in the CNS at the peak of the disease (Fig. 5C, Supplemental Fig. 4C, 4D) and as expected increased numbers of Helios⁺ Tregs expressing ST2 (Fig. 5D, Supplemental Fig. 4E).

Next, we wanted to exclude a potential DC-intrinsic defect during the priming phase in the absence of RelB and therefore adopted a protocol of Ab-mediated depletion of Tregs prior to EAE induction (57). As expected, Treg depletion aggravated disease scores in control animals (Fig. 5E). Despite the only moderate Treg depletion efficiency in RelB^{ADC} mice at the time of immunization and rapid Treg recovery at the peak of disease (Supplemental Fig. 4F, 4G), we observed similar disease scores in Treg-depleted RelB^{ADC} and control animals (Fig. 5E). This was again associated with an accumulation of pathogenic cytokine-producing T cells in the CNS (Fig. 5F). Thus, RelB-deficient DCs are capable of inducing a full-blown pathogenic immune response in the absence of an excess of polyclonal tissue Tregs. Notably, treatment of mice with rIL-33, which is known to boost accumulation of tissue Tregs, is equally able to reduce EAE disease scores (58). To address whether RelB^{ADC} mice support increased de novo production of self-reactive Tregs during EAE in vivo, we transferred sort-purified MOG-specific 2D2Fopx3⁺ naive T cells into RelB^{ADC} or control mice prior to EAE induction. Interestingly, 2D2 T cells started to upregulate Fopx3 in RelB^{ADC} but not control mice

FIGURE 4. Tregs from RelB^{ADC} mice are functional in vitro and in vivo but de novo induction of Tregs in the intestinal tract is impaired. **(A)** Proliferation index from an in vitro suppression assay with DCs and Teff cells isolated from WT mice and Tregs isolated from littermate control or RelB^{ADC} mice. **(B)** Six-day-old mice with the scurfy mutation received bulk CD4⁺ T cells isolated from littermate control or RelB^{ADC} mice by i.p. injection. Upper plot indicate survival rate, lower plot indicate mean percentage of initial body weight at day 20. **(C)** Littermate control and RelB^{ADC} mice received congenically labeled naive OT-II T cells by i.v. injection and were exposed to 1.5% chicken OVA containing drinking water for the following 9 d. Representative contour plots (left) and quantification (right) of Foxp3⁺ and ROR(γt)⁺Foxp3⁺ among OT-II cells isolated from the lamina propria of the small intestine are shown. **(D)** Comparison of endogenous and transferred T cells for Foxp3 and Gata3 expression among T cells isolated from the lamina propria of the small intestine from the experiment in (C). **(E)** Quantification of the data shown in (D). All data show pooled results of at least two independent experiments and were analyzed by two-tailed Student *t* test. Bar diagrams show mean ± SD. **p* < 0.05, ***p* < 0.01, ****p* < 0.001, *****p* < 0.0001.



by day 7 after immunization in the draining inguinal lymph node before any sign of disease onset (Fig. 5G). In summary, these data reveal a key role of tissue Tregs for preventing autoimmune inflammation, which can be achieved through selected deletion of the NF-κB family member RelB in DCs.

Discussion

APCs and notably DCs have been known as initiator cells for the induction of immune responses to foreign Ags, whereas their role for active tolerance induction with therapeutic potential has been recognized only at the beginning of this century (59). Particularly the mutual relationship between DCs and Tregs through increasing DC numbers and a simultaneous increase of Tregs indicates a critical role of DC–T cell interactions for dictating Treg populations (60). Treg homeostasis and function in the periphery is further dependent on continuous triggering of the TCR by (auto-) Ags most likely constantly presented by DCs. Yet, this effect is independent from Treg hallmarks like Treg signature gene expression or the ability to use IL-2 but alters expression of a number of tissue Treg-associated genes, including Helios and Gata3 (61, 62). In this study, we have identified one pathway within the DC compartment that limits the proliferation and therefore also accumulation of tissue Tregs: Ablation of RelB but not NF-κB2 within CD11c⁺ cells leads to a drastic increase in Treg numbers that predominantly show a tissue Treg phenotype. Most likely, the majority of such accumulated Helios⁺ Tregs in RelB^{ADC} mice are specific for self-antigens, as both thymic and tissue-restricted neo-self-antigens are able to induce Helios⁺ Tregs, whereas Treg-specific Helios expression has not been described in Tregs with TCR specificities for foreign Ags (48, 49). Thus, it remains possible that both enhanced generation of Tregs in the thymus and increased de novo generation in the periphery contribute to the increase in Tregs although the latter

possibility may be more relevant in RelB^{ADC} mice according to de novo Treg induction of 2D2 T cells (Fig. 5F) and low expression of Satb1 and Bcl2. Accumulated Tregs in RelB^{ADC} mice show hallmarks of tissue Tregs, including expression of ST2, Gata3, and Helios and are able to almost completely protect from autoimmune inflammation of the CNS. DCs have been previously associated with maintenance and induction of self-reactive Tregs. However, Batf3-dependent CD8α⁺ DCs were dispensable for the induction of prostate-specific Tregs (15). In line with these results, RelB^{ADC} mice show a reduction mainly in Sirpα⁺CD8α⁻ DCs but not CD8α⁺ (Batf3-dependent DCs) due to cell-intrinsic developmental defects in the absence of RelB (42, 43). This results in a dominant accumulation of DEC-205⁺ DCs that have been previously shown to be ideal targets for Ag-specific tolerance applications via induction of Foxp3⁺ Tregs (44). Notably, therapeutic targeting of MOG expression to DCs was able to induce PD-1⁺ Tregs and protect mice from EAE, whereas conditional ablation of DCs resulted in a more severe inflammation of the CNS (14).

Mechanistically, ST2 deficiency has been shown to prevent Gata3 expression in Tregs, and exogenous IL-33 is able to induce accumulation of ST2⁺ Tregs (8, 51, 63). However, accumulated tissue Tregs in RelB^{ADC} mice were independent from non-hematopoietic IL-33 and also neutralization of IL-33 by sST2 did not reduce Treg levels significantly although it remains possible that DCs themselves are able to provide IL-33 (e.g., within the immunological synapse for expansion of type 2-biased Tregs in RelB^{ADC} mice that we were unable to neutralize [Fig. 3] and [52, 64]). Noteworthy is that IL-33-deficient mice possess normal levels of ST2⁺ Tregs (54). This may indicate that IL-33 expands Tregs to prevent tissue damage (e.g., during ongoing type 2 immune-driven inflammation) but is not the primary driver for the tissue Treg phenotype under physiologic conditions. Alternatively,

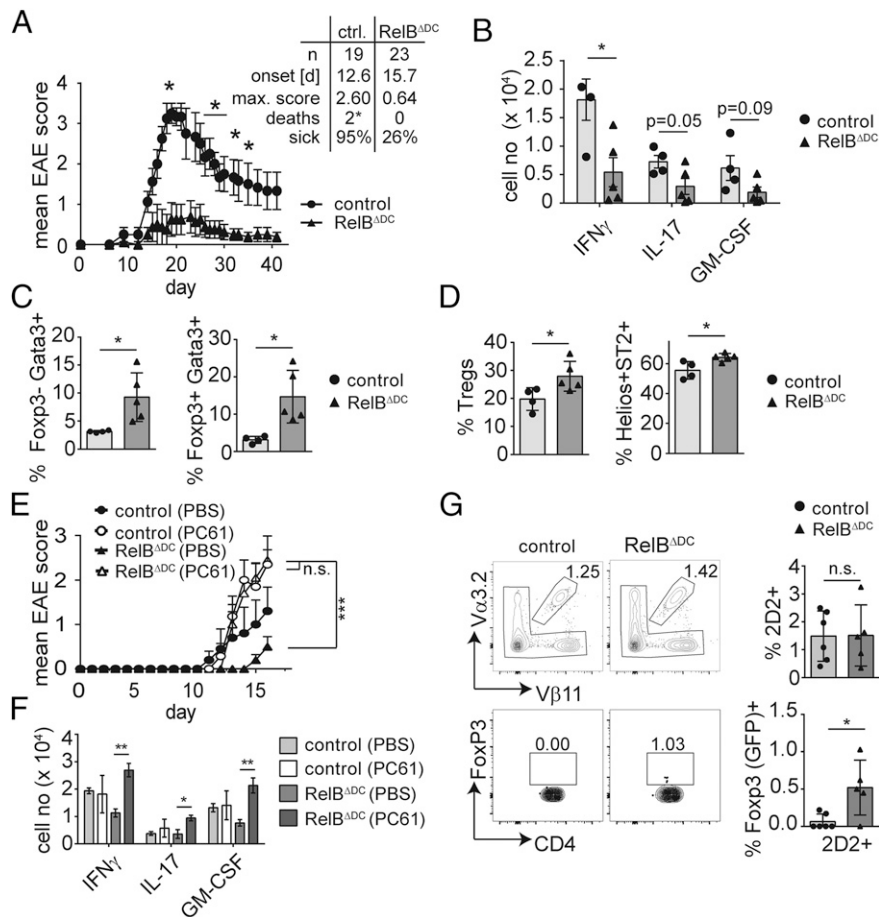


FIGURE 5. RelB^{ADC} mice are protected from EAE due to accumulation of Tregs. EAE was induced by immunizing littermate control or RelB^{ADC} mice with MOG_{35–55} in CFA as described in *Materials and Methods*. **(A)** EAE clinical score in WT and RelB^{ADC} mice shown as mean \pm SEM of one representative experiment. Table depicts summary of all experiments. Sick, score of at least one. Mice that had to be sacrificed because of high disease scores are indicated as deaths. **(B)** Total numbers of cytokine-expressing Th cells in the CNS at peak of disease after PMA/ionomycin restimulation of one representative experiment. **(C)** Frequency of Foxp3⁺ Gata3⁺ and Foxp3⁺ Gata3⁺ Th cells in the CNS at peak of disease. **(D)** Frequency of Foxp3⁺ cells within CD4⁺ T cells or frequency of Helios⁺ ST2⁺ cells within Foxp3⁺ Tregs in the CNS at peak of disease. **(E)** Clinical score of EAE in littermate control and RelB^{ADC} mice treated with an anti-CD25 Ab (open symbols) or PBS (filled symbols) prior induction of EAE as described in *Materials and Methods* section. Diagram shows mean \pm SEM. **(F)** Total cell number of cytokine-expressing Foxp3⁺ CD4⁺ T cells in the CNS at the peak of EAE. **(G)** Littermate control and RelB^{ADC} mice received 2.5×10^6 sort-purified MOG-specific Foxp3/GFP⁺ 2D2 T cells prior EAE induction via i.v. injection. Upper plots (left) and quantification (right) indicate frequency of V α 3.2⁺V β 11⁺ 2D2 cells among CD4⁺ T cells isolated from draining inguinal lymph nodes at day 8 after EAE induction. Lower plots indicate frequency (left) and quantification (right) of Foxp3/GFP⁺ cells among V α 3.2⁺V β 11⁺ 2D2 T cells isolated from draining inguinal lymph nodes at day 8 after EAE induction. Bar diagrams show mean \pm SD of at least two independent experiments unless otherwise indicated. Statistical analysis was performed using Mann-Whitney *U* test (in [A]) or two-way ANOVA with Tukey multiple correction test (in [E]). Otherwise, unpaired two-tailed Student *t* test was used. **p* < 0.05, ***p* < 0.01, ****p* < 0.001.

IL-2/anti-IL-2 Ab complexes are able to induce high numbers of Gata3-expressing Tregs, and activation of T cells by RelB-deficient DCs has been shown to result in increased IL-2 production by T cells or DCs (6, 63, 65), but we did not find any difference in systemic IL-2 or IL-33 cytokine levels in the serum or peritoneal lavage of RelB^{ADC} mice.

In line with their assumed specificity for self-antigens, tissue Tregs have been shown to regulate a number of physiological processes, including muscle repair, lung integrity after influenza infection, and metabolic disorders in fat tissues (10–12). We now demonstrate that increasing tissue Treg numbers through ablation of DC-intrinsic RelB is also able to prevent autoimmune inflammation (Fig. 5). Notably, treatment of mice with rIL-33, which among other effects is known to boost accumulation of tissue Tregs, is able to equally reduce EAE disease scores (58). It remains to be addressed how tissue Tregs could fulfill this task but three general possibilities seem plausible: First, tissue Tregs could modulate DCs to prevent effective priming toward bona-fide

self-antigens. This possibility has been proposed as a general concept for Treg function but could be dangerous for simultaneous immune responses of different origins and directed toward distinct specificities. Second, accumulation of tissue Tregs could enhance tissue integrity and prevent (e.g., break of the blood-brain barrier) as has been shown for other tissues like lung and muscle (11, 12). Finally, Tregs may prevent Ag-specific T cell responses directly. This would require expansion of de novo-induced Tregs (Fig. 5G) or necessitate the accumulation of MOG-specific Tregs at steady-state in RelB^{ADC} mice. How RelB deficiency in DCs can result in enhanced de novo induction and accumulation of self-reactive Tregs but at the same time result in impaired de novo to orally supplied, foreign Ags remains to be identified, but different functional programs exploited by different DC subsets adapted to their local environment and tissue function are likely in place.

Protection from autoimmune inflammation in RelB^{ADC} mice comes at a high cost, as we have observed impaired tolerance

induction in response to oral Ags and particularly in the numbers of ROR(γ)⁺ Tregs. This Treg subset is now seen as a major factor for tolerance of symbiotic microbes and is essential for the efficient suppression of different forms of colitis (2, 3, 66, 67). Interestingly, RelB^{ADC} mice show a type 2 bias both within the Treg and the Teff compartment in PEC and small intestine and also after oral Ag exposure. This may be attributed due to cell-intrinsic defects in tissue-resident DCs but also to the lower numbers of ROR(γ)⁺ Tregs counteracting type 2 immunity (2). Related to these results, DC-specific ablation of TRAF6, a key adaptor protein for the integration of TLR and some TNFR members into NF- κ B activation, leads to a spontaneous inflammation of the small intestine characterized by impaired Treg differentiation in response to oral Ag and a marked type 2 immune bias, including accumulation of Th2 cells and eosinophils (68). TRAF6 can also signal via the classical NF- κ B pathway, but recent evidence suggests that NF- κ B signaling in DCs cannot be strictly divided into classical and alternative signaling pathways (40). Our observation that deletion of NF- κ B2 in DCs did not fully recapitulate the RelB^{ADC} in terms of Treg accumulation (Fig. 2A) supports the importance of RelB/p50 or complexes or NF- κ B2 homodimers in DCs cross-regulation via classical NF- κ B pathways.

Full knockout of RelB results in a fulminant autoimmune inflammation that is dependent on the adaptive immune system (37). However, this can be attributed to the essential role of RelB in mTECs and as a consequence impaired negative selection (19). Indeed, patients suffering from RelB deficiency have to undergo hematopoietic stem cell transplantation due to severe immune deficiency (69). Noteworthy is that at least in one case increased frequencies of Tregs were observed in a RelB-deficient patient before hematopoietic stem cell transplantation (personal communication to Chaim Roifman, The Hospital for Sick Children, Toronto, Canada). Thus, increased Treg numbers cannot control autoimmune inflammation due to impaired central tolerance per se. The reasons for this observation may lay in potential differences and sources of respective self-antigens.

This observation supports our results that RelB could be an attractive target to enhance the number of tissue Tregs for the treatment of autoimmune diseases although not at zero cost. Indeed, infusion of RelB-silenced DCs have been used to treat ongoing myasthenia gravis and shown to prolong allograft tolerance, which was again associated with a Th2 and Treg bias (70–72). Likewise, transfer of WT DCs into RelB-deficient hosts has been shown to reverse airway inflammation and counteract the type 2 bias observed in these mice (73). Finally, type 2-biased Tregs have been found to accumulate in tumorigenic environments and may contribute to prevent effective antitumor immunity (74). Such “negative” functions of type 2 immune-biased Tregs may help to explain why the number of tissue Tregs is limited by RelB-dependent DCs. In summary, the inverse association of RelB-expressing DCs with the accumulation of Th2-biased tissue Tregs proves a dominant effect of tissue Treg numbers for effective protection from autoimmunity.

Acknowledgments

This work is dedicated to Falk Weih who regrettably departed from this life before the end of this study. He will be remembered as a passionate scientist, a wise group leader, and, first and foremost, a good friend. We thank Benjamin Schnautz and Johanna Grosch for technical assistance and Boris Reizis, Veit Buchholz, Dirk Baumjohann, and Ursula Zimmer-Strobl for providing mice.

Disclosures

The authors have no financial conflicts of interest.

References

- Josefowicz, S. Z., L. F. Lu, and A. Y. Rudensky. 2012. Regulatory T cells: mechanisms of differentiation and function. *Annu. Rev. Immunol.* 30: 531–564.
- Ohnmacht, C., J. H. Park, S. Cording, J. B. Wing, K. Atarashi, Y. Obata, V. Gaboriau-Routhiau, R. Marques, S. Dulauroy, M. Fedoseeva, et al. 2015. MUCOSAL IMMUNOLOGY. The microbiota regulates type 2 immunity through ROR γ ⁺ T cells. *Science* 349: 989–993.
- Sefik, E., N. Geva-Zatorsky, S. Oh, L. Konnikova, D. Zemmour, A. M. McGuire, D. Burzyn, A. Ortiz-Lopez, M. Lobera, J. Yang, et al. 2015. MUCOSAL IMMUNOLOGY. Individual intestinal symbionts induce a distinct population of ROR γ ⁺ regulatory T cells. *Science* 349: 993–997.
- Levine, A. G., A. Mendoza, S. Hemmers, B. Moltedo, R. E. Niec, M. Schizas, B. E. Hoyos, E. V. Putintseva, A. Chaudhry, S. Dikiy, et al. 2017. Stability and function of regulatory T cells expressing the transcription factor T-bet. [Published erratum appears in 2017 *Nature* 550: 142.] *Nature* 546: 421–425.
- Koch, M. A., G. Tucker-Heard, N. R. Perdue, J. R. Killebrew, K. B. Urdahl, and D. J. Campbell. 2009. The transcription factor T-bet controls regulatory T cell homeostasis and function during type 1 inflammation. *Nat. Immunol.* 10: 595–602.
- Wohlfert, E. A., J. R. Grainger, N. Bouladoux, J. E. Konkel, G. Oldenhove, C. H. Ribeiro, J. A. Hall, R. Yagi, S. Naik, R. Bhairavabhotla, et al. 2011. GATA3 controls Foxp3⁺ regulatory T cell fate during inflammation in mice. *J. Clin. Invest.* 121: 4503–4515.
- Yu, F., S. Sharma, J. Edwards, L. Feigenbaum, and J. Zhu. 2015. Dynamic expression of transcription factors T-bet and GATA-3 by regulatory T cells maintains immunotolerance. *Nat. Immunol.* 16: 197–206.
- Delacher, M., C. D. Imbusch, D. Weichenhan, A. Breiling, A. Hotz-Wagenblatt, U. Träger, A. C. Hofer, D. Kägebein, Q. Wang, F. Frauhammer, et al. 2017. Genome-wide DNA-methylation landscape defines specialization of regulatory T cells in tissues. [Published erratum appears in 2017 *Nat. Immunol.* 18: 1361.] *Nat. Immunol.* 18: 1160–1172.
- Panduro, M., C. Benoist, and D. Mathis. 2016. Tissue Tregs. *Annu. Rev. Immunol.* 34: 609–633.
- Vasanthakumar, A., K. Moro, A. Xin, Y. Liao, R. Gloury, S. Kawamoto, S. Fagarasan, L. A. Mielke, S. Afshar-Sterle, S. L. Masters, et al. 2015. The transcriptional regulators IRF4, BATF and IL-33 orchestrate development and maintenance of adipose tissue-resident regulatory T cells. [Published erratum appears in 2015 *Nat. Immunol.* 16: 544.] *Nat. Immunol.* 16: 276–285.
- Arpaia, N., J. A. Green, B. Moltedo, A. Arvey, S. Hemmers, S. Yuan, P. M. Treuting, and A. Y. Rudensky. 2015. A distinct function of regulatory T cells in tissue protection. *Cell* 162: 1078–1089.
- Burzyn, D., W. Kuswanto, D. Kolodin, J. L. Shadrach, M. Cerletti, Y. Jang, E. Sefik, T. G. Tan, A. J. Wagers, C. Benoist, and D. Mathis. 2013. A special population of regulatory T cells potentiates muscle repair. *Cell* 155: 1282–1295.
- Wynn, T. A. 2015. Type 2 cytokines: mechanisms and therapeutic strategies. *Nat. Rev. Immunol.* 15: 271–282.
- Yogev, N., F. Frommer, D. Lukas, K. Kautz-Neu, K. Karram, D. Ielo, E. von Stebut, H. C. Probst, M. van den Broek, D. Riethmacher, et al. 2012. Dendritic cells ameliorate autoimmunity in the CNS by controlling the homeostasis of PD-1 receptor(+) regulatory T cells. *Immunity* 37: 264–275.
- Leventhal, D. S., D. C. Gilmore, J. M. Berger, S. Nishi, V. Lee, S. Malchow, D. E. Kline, J. Kline, D. J. Vander Griend, H. Huang, et al. 2016. Dendritic cells coordinate the development and homeostasis of organ-specific regulatory T cells. *Immunity* 44: 847–859.
- Ohnmacht, C., A. Pullner, S. B. King, I. Drexler, S. Meier, T. Brocker, and D. Voehringer. 2009. Constitutive ablation of dendritic cells breaks self-tolerance of CD4 T cells and results in spontaneous fatal autoimmunity. *J. Exp. Med.* 206: 549–559.
- Birnberg, T., L. Bar-On, A. Sapozhnikov, M. L. Caton, L. Cervantes-Barragán, D. Makia, R. Krauthgamer, O. Brenner, B. Ludewig, D. Brockschneider, et al. 2008. Lack of conventional dendritic cells is compatible with normal development and T cell homeostasis, but causes myeloid proliferative syndrome. *Immunity* 29: 986–997.
- Esterházy, D., J. Loschko, M. London, V. Jove, T. Y. Oliveira, and D. Mucida. 2016. Classical dendritic cells are required for dietary antigen-mediated induction of peripheral T(reg) cells and tolerance. *Nat. Immunol.* 17: 545–555.
- Riemann, M., N. Andreas, M. Fedoseeva, E. Meier, D. Weih, H. Freytag, R. Schmidt-Ullrich, U. Klein, Z. Q. Wang, and F. Weih. 2017. Central immune tolerance depends on crosstalk between the classical and alternative NF- κ B pathways in medullary thymic epithelial cells. *J. Autoimmun.* 81: 56–67.
- Ishikawa, H., D. Carrasco, E. Claudio, R. P. Ryseck, and R. Bravo. 1997. Gastric hyperplasia and increased proliferative responses of lymphocytes in mice lacking the COOH-terminal ankyrin domain of NF-kappaB2. *J. Exp. Med.* 186: 999–1014.
- Pichery, M., E. Mirey, P. Mercier, E. Lefrancais, A. Dujardin, N. Ortega, and J. P. Girard. 2012. Endogenous IL-33 is highly expressed in mouse epithelial barrier tissues, lymphoid organs, brain, embryos, and inflamed tissues: in situ analysis using a novel Il-33-LacZ gene trap reporter strain. *J. Immunol.* 188: 3488–3495.
- Bettelli, E., Y. Carrier, W. Gao, T. Korn, T. B. Strom, M. Oukka, H. L. Weiner, and V. K. Kuchroo. 2006. Reciprocal developmental pathways for the generation of pathogenic effector TH17 and regulatory T cells. *Nature* 441: 235–238.
- Bettelli, E., M. Pagany, H. L. Weiner, C. Linington, R. A. Sobel, and V. K. Kuchroo. 2003. Myelin oligodendrocyte glycoprotein-specific T cell

- receptor transgenic mice develop spontaneous autoimmune optic neuritis. *J. Exp. Med.* 197: 1073–1081.
24. Barden, M. J., J. Allison, W. R. Heath, and F. R. Carbone. 1998. Defective TCR expression in transgenic mice constructed using cDNA-based alpha- and beta-chain genes under the control of heterologous regulatory elements. *Immunol. Cell Biol.* 76: 34–40.
 25. Caton, M. L., M. R. Smith-Raska, and B. Reizis. 2007. Notch-RBP-J signaling controls the homeostasis of CD8⁺ dendritic cells in the spleen. *J. Exp. Med.* 204: 1653–1664.
 26. De Silva, N. S., K. Silva, M. M. Anderson, G. Bhagat, and U. Klein. 2016. Impairment of mature B cell maintenance upon combined deletion of the alternative NF- κ B transcription factors RELB and NF- κ B2 in B cells. *J. Immunol.* 196: 2591–2601.
 27. Zhou, X., L. T. Jeker, B. T. Fife, S. Zhu, M. S. Anderson, M. T. McManus, and J. A. Bluestone. 2008. Selective miRNA disruption in T reg cells leads to uncontrolled autoimmunity. *J. Exp. Med.* 205: 1983–1991.
 28. Soza-Ried, C., C. C. Bleul, M. Schorpp, and T. Boehm. 2008. Maintenance of thymic epithelial phenotype requires extrinsic signals in mouse and zebrafish. *J. Immunol.* 181: 5272–5277.
 29. Wan, Y. Y., and R. A. Flavell. 2005. Identifying Foxp3-expressing suppressor T cells with a bicistronic reporter. *Proc. Natl. Acad. Sci. USA* 102: 5126–5131.
 30. Brunkow, M. E., E. W. Jeffery, K. A. Hjerrild, B. Paepel, L. B. Clark, S. A. Yasayko, J. E. Wilkinson, D. Galas, S. F. Ziegler, and F. Ramsdell. 2001. Disruption of a new forkhead/winged-helix protein, scurf1, results in the fatal lymphoproliferative disorder of the scurfy mouse. *Nat. Genet.* 27: 68–73.
 31. Wu, T. D., and S. Nacu. 2010. Fast and SNP-tolerant detection of complex variants and splicing in short reads. *Bioinformatics* 26: 873–881.
 32. DeLuca, D. S., J. Z. Levin, A. Sivachenko, T. Fennell, M. D. Nazaire, C. Williams, M. Reich, W. Winckler, and G. Getz. 2012. RNA-SeqQC: RNA-seq metrics for quality control and process optimization. *Bioinformatics* 28: 1530–1532.
 33. Liao, Y., G. K. Smyth, and W. Shi. 2014. FeatureCounts: an efficient general purpose program for assigning sequence reads to genomic features. *Bioinformatics* 30: 923–930.
 34. Love, M. I., W. Huber, and S. Anders. 2014. Moderated estimation of fold change and dispersion for RNA-seq data with DESeq2. *Genome Biol.* 15: 550.
 35. Weih, F., D. Carrasco, S. K. Durham, D. S. Barton, C. A. Rizzo, R. P. Ryseck, S. A. Lira, and R. Bravo. 1995. Multiorgan inflammation and hematopoietic abnormalities in mice with a targeted disruption of RelB, a member of the NF- κ B/Rel family. *Cell* 80: 331–340.
 36. Weih, F., S. K. Durham, D. S. Barton, W. C. Sha, D. Baltimore, and R. Bravo. 1996. Both multiorgan inflammation and myeloid hyperplasia in RelB-deficient mice are T cell dependent. *J. Immunol.* 157: 3974–3979.
 37. Barton, D., H. HogenEsch, and F. Weih. 2000. Mice lacking the transcription factor RelB develop T cell-dependent skin lesions similar to human atopic dermatitis. *Eur. J. Immunol.* 30: 2323–2332.
 38. Grinberg-Bleyer, Y., R. Caron, J. J. Seeley, N. S. De Silva, C. W. Schindler, M. S. Hayden, U. Klein, and S. Ghosh. 2018. The alternative NF- κ B pathway in regulatory T cell homeostasis and suppressive function. *J. Immunol.* 200: 2362–2371.
 39. Li, J., S. Chen, W. Chen, Q. Ye, Y. Dou, Y. Xiao, L. Zhang, L. J. Minze, X. C. Li, and X. Xiao. 2018. Role of the NF- κ B family member RelB in regulation of Foxp3⁺ regulatory T cells in vivo. *J. Immunol.* 200: 1325–1334.
 40. Shih, V. F., J. Davis-Turak, M. Macal, J. Q. Huang, J. Ponomarenko, J. D. Kearns, T. Yu, R. Fagerlund, M. Asagiri, E. I. Zuniga, and A. Hoffmann. 2012. Control of RelB during dendritic cell activation integrates canonical and noncanonical NF- κ B pathways. *Nat. Immunol.* 13: 1162–1170.
 41. Wu, L., A. D'Amico, K. D. Winkel, M. Suter, D. Lo, and K. Shortman. 1998. RelB is essential for the development of myeloid-related CD8 α dendritic cells but not of lymphoid-related CD8 α dendritic cells. *Immunity* 9: 839–847.
 42. Briseño, C. G., M. Gargaro, V. Durai, J. T. Davidson, D. J. Theisen, D. A. Anderson, III, D. V. Novack, T. L. Murphy, and K. M. Murphy. 2017. Deficiency of transcription factor RelB perturbs myeloid and DC development by hematopoietic-extrinsic mechanisms. *Proc. Natl. Acad. Sci. USA* 114: 3957–3962.
 43. Andreas, N., M. Riemann, C. N. Castro, M. Groth, I. Koliesnik, C. Engelmann, T. Sparwasser, T. Kamradt, R. Haenold, and F. Weih. 2018. A new RelB-dependent CD117⁺ CD172a⁺ murine DC subset preferentially induces Th2 differentiation and supports airway hyperresponses in vivo. *Eur. J. Immunol.* 48: 923–936.
 44. Kretschmer, K., I. Apostolou, D. Hawiger, K. Khazaie, M. C. Nussenzweig, and H. von Boehmer. 2005. Inducing and expanding regulatory T cell populations by foreign antigen. *Nat. Immunol.* 6: 1219–1227.
 45. Proietto, A. I., S. van Dommelen, P. Zhou, A. Rizzitelli, A. D'Amico, R. J. Steptoe, S. H. Naik, M. H. Lahoud, Y. Liu, P. Zheng, et al. 2008. Dendritic cells in the thymus contribute to T-regulatory cell induction. [Published erratum appears in 2009 *Proc. Natl. Acad. Sci. USA* 106: 1679.] *Proc. Natl. Acad. Sci. USA* 105: 19869–19874.
 46. Li, J., J. Park, D. Foss, and I. Goldschneider. 2009. Thymus-homing peripheral dendritic cells constitute two of the three major subsets of dendritic cells in the steady-state thymus. *J. Exp. Med.* 206: 607–622.
 47. Thiault, N., J. Darrigues, V. Adoue, M. Gros, B. Binet, C. Perals, B. Leobon, N. Fazilleau, O. P. Joffre, E. A. Robey, et al. 2015. Peripheral regulatory T lymphocytes recirculating to the thymus suppress the development of their precursors. *Nat. Immunol.* 16: 628–634.
 48. Kieback, E., E. Hilgenberg, U. Stervbo, V. Lampropoulou, P. Shen, M. Bunse, Y. Jaimes, P. Boudinot, A. Radbruch, U. Klemm, et al. 2016. Thymus-derived regulatory T cells are positively selected on natural self-antigen through cognate interactions of high functional avidity. *Immunity* 44: 1114–1126.
 49. Legoux, F. P., J. B. Lim, A. W. Cauley, S. Dikly, J. Ertelt, T. J. Mariani, T. Sparwasser, S. S. Way, and J. J. Moon. 2015. CD4⁺ T cell tolerance to tissue-restricted self antigens is mediated by antigen-specific regulatory T cells rather than deletion. *Immunity* 43: 896–908.
 50. Kitagawa, Y., N. Ohkura, Y. Kidani, A. Vandenbon, K. Hirota, R. Kawakami, K. Yasuda, D. Motooka, S. Nakamura, M. Kondo, et al. 2017. Guidance of regulatory T cell development by Satb1-dependent super-enhancer establishment. [Published erratum appears in 2017 *Nat. Immunol.* 18: 474.] *Nat. Immunol.* 18: 173–183.
 51. Schiering, C., T. Krausgruber, A. Chomka, A. Fröhlich, K. Adelmann, E. A. Wohlfert, J. Pott, T. Griseri, J. Bollrath, A. N. Hegazy, et al. 2014. The alarmin IL-33 promotes regulatory T-cell function in the intestine. *Nature* 513: 564–568.
 52. Chen, C. C., T. Kobayashi, K. Iijima, F. C. Hsu, and H. Kita. 2017. IL-33 dysregulates regulatory T cells and impairs established immunologic tolerance in the lungs. *J. Allergy Clin. Immunol.* 140: 1351–1363.e7.
 53. Liew, F. Y., J. P. Girard, and H. R. Turnquist. 2016. Interleukin-33 in health and disease. *Nat. Rev. Immunol.* 16: 676–689.
 54. Siede, J., A. Fröhlich, A. Datsi, A. N. Hegazy, D. V. Varga, V. Holescka, H. Saito, S. Nakae, and M. Löhning. 2016. IL-33 receptor-expressing regulatory T cells are highly activated, Th2 biased and suppress CD4 T cell proliferation through IL-10 and TGF β release. *PLoS One* 11: e0161507.
 55. Noval Rivas, M., O. T. Burton, P. Wise, L. M. Charbonnier, P. Georgiev, H. C. Oettgen, R. Rachid, and T. A. Chatila. 2015. Regulatory T cell reprogramming toward a Th2-cell-like lineage impairs oral tolerance and promotes food allergy. *Immunity* 42: 512–523.
 56. Kim, K. S., S. W. Hong, D. Han, J. Yi, J. Jung, B. G. Yang, J. Y. Lee, M. Lee, and C. D. Surh. 2016. Dietary antigens limit mucosal immunity by inducing regulatory T cells in the small intestine. *Science* 351: 858–863.
 57. Korn, T., M. Mitsdoerffer, A. L. Croxford, A. Awasthi, V. A. Dardalhon, G. Galileos, P. Vollmar, G. L. Stritesky, M. H. Kaplan, A. Waisman, et al. 2008. IL-6 controls Th17 immunity in vivo by inhibiting the conversion of conventional T cells into Foxp3⁺ regulatory T cells. *Proc. Natl. Acad. Sci. USA* 105: 18460–18465.
 58. Jiang, H. R., M. Milovanović, D. Allan, W. Niedbala, A. G. Besnard, S. Y. Fukada, J. C. Alves-Filho, D. Togbe, C. S. Goodyear, C. Linington, et al. 2012. IL-33 attenuates EAE by suppressing IL-17 and IFN- γ production and inducing alternatively activated macrophages. *Eur. J. Immunol.* 42: 1804–1814.
 59. Hawiger, D., K. Inaba, Y. Dorsett, M. Guo, K. Mahnke, M. Rivera, J. V. Ravetch, R. M. Steinman, and M. C. Nussenzweig. 2001. Dendritic cells induce peripheral T cell unresponsiveness under steady state conditions in vivo. *J. Exp. Med.* 194: 769–779.
 60. Darrasse-Jèze, G., S. Deroubaix, H. Mouquet, G. D. Victora, T. Eisenreich, K. H. Yao, R. F. Masilamani, M. L. Dustin, A. Rudensky, K. Liu, and M. C. Nussenzweig. 2009. Feedback control of regulatory T cell homeostasis by dendritic cells in vivo. *J. Exp. Med.* 206: 1853–1862.
 61. Vahl, J. C., C. Drees, K. Heger, S. Heink, J. C. Fischer, J. Nedjic, N. Ohkura, H. Morikawa, H. Poeck, S. Schallenberg, et al. 2014. Continuous T cell receptor signals maintain a functional regulatory T cell pool. *Immunity* 41: 722–736.
 62. Levine, A. G., A. Arvey, W. Jin, and A. Y. Rudensky. 2014. Continuous requirement for the TCR in regulatory T cell function. *Nat. Immunol.* 15: 1070–1078.
 63. Matta, B. M., J. M. Lott, L. R. Mathews, Q. Liu, B. R. Rosborough, B. R. Blazar, and H. R. Turnquist. 2014. IL-33 is an unconventional Alarmin that stimulates IL-2 secretion by dendritic cells to selectively expand IL-33R/ST2⁺ regulatory T cells. *J. Immunol.* 193: 4010–4020.
 64. Williams, J. W., M. Y. Tjota, B. S. Clay, B. Vander Lugt, H. S. Bandukwala, C. L. Hrusch, D. C. Decker, K. M. Blaine, B. R. Fixsen, H. Singh, et al. 2013. Transcription factor IRF4 drives dendritic cells to promote Th2 differentiation. *Nat. Commun.* 4: 2990.
 65. Döhler, A., T. Schneider, I. Eckert, E. Ribechini, N. Andreas, M. Riemann, B. Reizis, F. Weih, and M. B. Lutz. 2017. RelB⁺ steady-state migratory dendritic cells control the peripheral pool of the natural Foxp3⁺ regulatory T cells. *Front. Immunol.* 8: 726.
 66. Yang, B. H., S. Hagemann, P. Mamarelli, U. Lauer, U. Hoffmann, M. Beckstette, L. Föhse, I. Prinz, J. Pezoldt, S. Suerbaum, et al. 2016. Foxp3(+) T cells expressing ROR γ t represent a stable regulatory T-cell effector lineage with enhanced suppressive capacity during intestinal inflammation. *Mucosal Immunol.* 9: 444–457.
 67. Xu, M., M. Pokrovskii, Y. Ding, R. Yi, C. Au, O. J. Harrison, C. Galan, Y. Belkaid, R. Bonneau, and D. R. Littman. 2018. c-MAF-dependent regulatory T cells mediate immunological tolerance to a gut pathobiont. [Published erratum appears in 2019 *Nature* 566: E7.] *Nature* 554: 373–377.
 68. Han, D., M. C. Walsh, P. J. Cejas, N. N. Dang, Y. F. Kim, J. Kim, L. Charrier-Hisamuddin, L. Chau, Q. Zhang, K. Bittinger, et al. 2013. Dendritic cell expression of the signaling molecule TRAF6 is critical for gut microbiota-dependent immune tolerance. *Immunity* 38: 1211–1222.
 69. Ovadia, A., Y. Dinur Schejter, E. Grunebaum, V. H. Kim, B. Reid, T. Schechter, E. Pope, and C. M. Roifman. 2017. Hematopoietic stem cell transplantation for RelB deficiency. *J. Allergy Clin. Immunol.* 140: 1199–1201.e3.
 70. Li, M., X. Zhang, X. Zheng, D. Lian, Z. X. Zhang, W. Ge, J. Yang, C. Vladau, M. Suzuki, D. Chen, et al. 2007. Immune modulation and tolerance induction by RelB-silenced dendritic cells through RNA interference. *J. Immunol.* 178: 5480–5487.

71. Yang, H., Y. Zhang, M. Wu, J. Li, W. Zhou, G. Li, X. Li, B. Xiao, and P. Christodoss. 2010. Suppression of ongoing experimental autoimmune myasthenia gravis by transfer of RelB-silenced bone marrow dendritic cells is associated with a change from a T helper Th17/Th1 to a Th2 and FoxP3+ regulatory T-cell profile. *Inflamm. Res.* 59: 197–205.
72. Zhu, H. C., T. Qiu, X. H. Liu, W. C. Dong, X. D. Weng, C. H. Hu, Y. L. Kuang, R. H. Gao, C. Dan, and T. Tao. 2012. Tolerogenic dendritic cells generated by RelB silencing using shRNA prevent acute rejection. *Cell. Immunol.* 274: 12–18.
73. Nair, P. M., M. R. Starkey, T. J. Haw, R. Ruscher, G. Liu, M. R. Maradana, R. Thomas, B. J. O'Sullivan, and P. M. Hansbro. 2018. RelB-deficient dendritic cells promote the development of spontaneous allergic airway inflammation. *Am. J. Respir. Cell Mol. Biol.* 58: 352–365.
74. Halim, L., M. Romano, R. McGregor, I. Correa, P. Pavlidis, N. Grageda, S. J. Hoong, M. Yuksel, W. Jassem, R. F. Hannen, et al. 2017. An atlas of human regulatory T helper-like cells reveals features of Th2-like tregs that support a tumorigenic environment. *Cell Rep.* 20: 757–770.